

Article

The Steroid Saponin Protodioscin Modulates *Arabidopsis thaliana* Root Morphology Altering Auxin Homeostasis, Transport and Distribution

Ana Luiza Santos Wagner¹, Fabrizio Araniti² , Leonardo Bruno³, Emy Luiza Ishii-Iwamoto^{1,*} and Maria Rosa Abenavoli^{4,*}

¹ Laboratory of Biological Oxidations, Department of Biochemistry, State University of Maringa, Maringa 87020900, Brazil; analuizawagner@hotmail.com

² Department of Agricultural and Environmental Sciences (DISAA), University of Milan, Via Celoria, 20133 Milano, Italy; fabrizio.araniti@unimi.it

³ Department of Biology, Ecology and Soil Science, University of Calabria, Arcavacata di Rende (CS), 87036 Arcavacata di Rende, Italy; leonardo.bruno@unical.it

⁴ Department of Agriculture, University of Reggio di Calabria, 89124 Reggio Calabria, Italy

* Correspondence: eliiwamoto@uem.br (E.L.I.-I.); mrabenavoli@unirc.it (M.R.A.);
Tel.: +55-44-3011-4896 (E.L.I.-I.); +39-096-5169-4350 (M.R.A.)



Citation: Santos Wagner, A.L.; Araniti, F.; Bruno, L.; Ishii-Iwamoto, E.L.; Abenavoli, M.R. The Steroid Saponin Protodioscin Modulates *Arabidopsis thaliana* Root Morphology Altering Auxin Homeostasis, Transport and Distribution. *Plants* **2021**, *10*, 1600. <https://doi.org/10.3390/plants10081600>

Academic Editors: Per Kudsk and Simon Hodge

Received: 26 June 2021

Accepted: 29 July 2021

Published: 4 August 2021

Publisher's Note: MDPI stays neutral with regard to jurisdictional claims in published maps and institutional affiliations.



Copyright: © 2021 by the authors. Licensee MDPI, Basel, Switzerland. This article is an open access article distributed under the terms and conditions of the Creative Commons Attribution (CC BY) license (<https://creativecommons.org/licenses/by/4.0/>).

Abstract: To date, synthetic herbicides are the main tools used for weed control, with consequent damage to both the environment and human health. In this respect, searching for new natural molecules and understanding their mode of action could represent an alternative strategy or support to traditional management methods for sustainable agriculture. Protodioscin is a natural molecule belonging to the class of steroid saponins, mainly produced by monocotyledons. In the present paper, protodioscin's phytotoxic potential was assessed to identify its target and the potential mode of action in the model plant *Arabidopsis thaliana*. The results highlighted that the root system was the main target of protodioscin, which caused a high inhibitory effect on the primary root length (ED_{50} 50 μ M) with morphological alteration, accompanied by a significant increase in the lateral root number and root hair density. Through a pharmacological and microscopic approach, it was underlined that this saponin modified both auxin distribution and transport, causing an auxin accumulation in the region of root maturation and an alteration of proteins responsible for the auxin efflux (PIN2). In conclusion, the saponin protodioscin can modulate the root system of *A. thaliana* by interfering with the auxin transport (PAT).

Keywords: allelopathy; saponin; natural herbicide; specialized metabolites; phytotoxicity; auxin transport; root morphology

1. Introduction

Weeds are one of the major constraints for crop yield and quality due to the competition for water, light, and nutrients [1], showing high germination capacity, growth, and reproduction, even under adverse conditions [2]. To date, synthetic herbicide use is increasing since, due to their easy application and greater accessibility to farmers, they remain the most effective method for weed control [3]. However, their low biodegradability and persistence in agri-food products are the main causes of environmental pollution, food contamination, and human health injuries [4]. The intensive and indiscriminate use of herbicides has favoured the appearance of highly herbicide-resistant weed biotypes. There are currently 514 confirmed cases of resistant biotypes in 70 countries, among 262 species (152 dicotyledons and 110 monocotyledons), covering 23 of the 26 known herbicide sites of action [5].

Therefore, in past decades, the research has been focused on developing novel methods to limit or minimize these chemicals' utilization [6]. Natural compounds, generally

belonging to the secondary plant metabolism, offer potential advantages for seeking new molecules that are less harmful, easily degradable, structurally diverse, and target novel sites, compared to synthetic herbicides [7–9]. Therefore, they could be considered potential sources of new bioherbicides and/or as possible templates to develop novel agrochemicals [10–12]. Among these, coumarins, terpenoids, phenolic acids, and flavonoids, derived from plant residues or alive plant species with allelopathic properties and high biological activity, seem the most important source of bio-herbicides for weed control [7]. These compounds can directly or indirectly affect many physiological processes, such as cell division and elongation [13], nutrient uptake [14,15], photosynthesis [16–18], respiration [19] and hormone balance [20,21], by inducing different phenotypic responses [22,23].

The plant root system could be considered the first target of allelochemicals, which can modify its morphology and architecture in many plant species [20,24,25]. For example, the sesquiterpene farnesene strongly modified root morphology and anatomy, causing cellular damage, anisotropic growth, bold roots and a “left-handedness” phenotype in *Arabidopsis thaliana* (L.) Heynh. [26]. Coumarin strongly affected root morphology, causing a primary root reduction and increasing lateral root number and root hair length in *Arabidopsis* seedlings [27]. Similar results were observed with monoterpene citral [28], sesquiterpenoid nerolidol [20], alkaloid norharmane [25], and momilactone B [29]. All the authors suggested that these allelochemicals might alter the root system, affecting both the auxin signalling pathway and transport, and interfering with its spatio-temporal homeostasis.

Auxin plays a pivotal role in regulating root system growth and development by regulating cell division, differentiation and elongation, lateral root formation, gravitropic responses, and microtubule disorganization [30–33]. For example, the allelochemical benzoic acid inhibited primary root growth by increasing auxin accumulation in root tips and raising auxin biosynthesis and auxin polar transporters (PAT), AUX1 and PIN2, genes expression [24].

The involvement of specialized metabolites on plant growth and development and their influence on plant hormone homeostasis, especially auxin, has been widely documented [28,34]. Several studies demonstrated that quite a lot of secondary metabolites could modify root phenotype, altering auxin biosynthesis, signalling and/or transport. Among them, coumarin caused an alteration in root morphology, interacting with polar auxin transport (PAT) and modulating the influx or/and efflux proteins [27]. The coumarin derivative 4-methylumbelliferone was found to inhibit primary root growth and regulate lateral root formation by altering auxin redistribution [35]. By contrast, scopoletin, with a chemical structure similar to auxinic herbicide 2,4-D, fit into the auxin-binding site TIR1, exerting an auxin-like effect [36]. Moreover, the alkaloids narciclasine and norharmane significantly altered *Arabidopsis* growth, modulating auxin transport and inhibiting its biosynthesis [21,25,37,38].

Similar to auxin, reactive oxygen species (ROS) are often associated with root morphology alteration [39]. ROS accumulation can affect root growth [40], microtubule organization [26], and root hair formation [41]. Further, cross-talk between ROS and auxin to modulate root system elongation was already demonstrated [42,43].

Despite research efforts in secondary metabolites/auxin/ROS interaction, limited information is available concerning the saponin class.

The natural molecule protodioscin is a steroidal saponin commonly produced by monocotyledon species, such as different species belonging to the *Urochloa* and *Tribulus* genera [44,45]. In particular, *Urochloa ruziziensis* (R. Germ. and C. M. Evrard), a forage crop widely used as a cover plant in a non-till system, can reduce weed emergence in the field [46] and greenhouse [47]. This effect is attributable to protodioscin, which was identified in the butanol extract of *U. ruziziensis* straw [48]. Nepomuceno et al. [49] reported that protodioscin isolated from *U. ruziziensis* also inhibits the growth of *Glycine max* (L.) Merr. seedlings in laboratory conditions. Despite reports on the phytotoxicity of protodioscin, its mechanisms of action have not yet been elucidated. A disturbance in mitochondrial respiratory activity and an oxidative stress condition was demonstrated in the primary

roots of *Bidens pilosa* L. treated with protodioscin [50]. Recently, we demonstrated that the dicot *Ipomoea grandifolia* (Dammer) O'Donnell and the monocot *Digitaria insularis* (L.) Fedde weed treated with protodioscin and butanolic extract of *U. ruziziensis* have drastic alterations in root morphology, including a reduction in the primary root length, the precocious appearance of lateral roots and reduction in root hairs [51]. The roots also exhibited features of advanced cell differentiation in the vascular cylinder. Although these morphogenic responses have suggested a disturbance in the auxin signalling, no direct evidence for this hypothesis has been examined [51].

In this respect, the present paper provides a deep insight into the protodioscin effects on *Arabidopsis* roots, a model species sensitive to secondary metabolites [52], to understand its mode of action through a physiological, biochemical, and pharmacological approach. The critical role played by the phytohormone auxin in the protodioscin-mediated effect is particularly investigated.

2. Results

2.1. Dose-Response Curves

Although there is not a clear inhibitory effect at the lowest concentrations (15.6 and 31.3 μM), protodioscin significantly affected *A. thaliana* root growth, mainly at the concentration range of 62.5–500 μM , reducing the primary root length up to 85% (500 μM) (Figure 1A). The fitting of the raw data relating to this parameter, through non-linear regression, allowed to estimate the ED_{50} value equal to 50 μM (Figure 1A), the concentration adopted in the subsequent experiments.

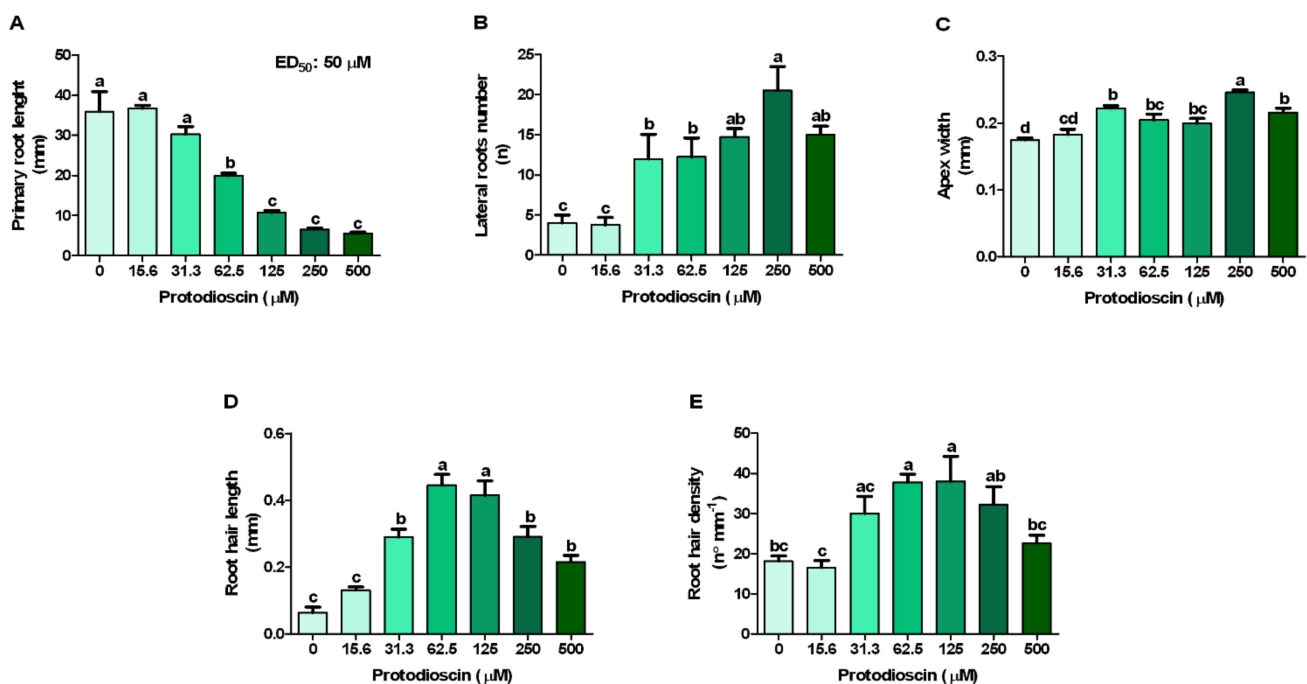


Figure 1. *Arabidopsis* roots morphology in response to the increasing doses of protodioscin: (A) primary root length; (B) lateral roots number; (C) apex width; (D) root hair length, and (E) root hair density. ED_{50} : dose causing 50% reduction of primary root length. Different letters indicate significant differences observed among treatments at $p \leq 0.05$ (SNK's test). $N = 4$.

At the lowest concentration (15.6 μM), protodioscin did not affect the number of the lateral roots, but it induced a strong stimulatory effect (2.5 times greater than the control) at 125 μM , reaching the maximum value at 250 μM (4 times greater than the control). Conversely, at the highest protodioscin concentration (500 μM), this positive effect was less marked (Figure 1B).

A similar trend was observed for apex width, for which protodioscin caused a thickening of the meristematic root area first detected at 31.3 μM (27% greater than the control) up to 250 μM (41%), after which its effect decreased again (23%, at 500 μM) (Figure 1C). Conversely, the root hair length and density were characterized by a gradual increase, reaching the maximum value at 62.5 and 125 μM , respectively, followed by a gradual reduction at the highest protodioscin concentration (Figure 1D,E, respectively). Root images confirmed the above results (Figure 2).

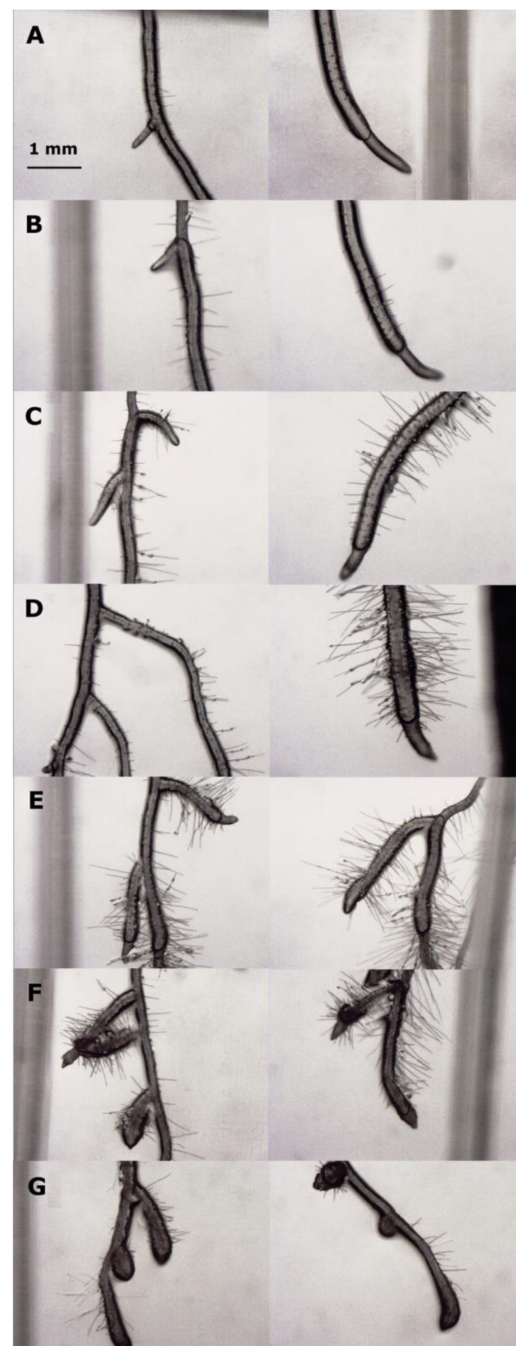


Figure 2. Stereoscopic microscopy images of *Arabidopsis* roots exposed to increasing doses of protodioscin: (A) control (0 μM); (B) 15.6 μM ; (C) 31.3 μM ; (D) 62.5 μM ; (E) 125 μM ; (F) 250 μM and (G) 500 μM . Scale bar 1 mm.

2.2. Protodioscin and Natural/Synthetic Auxin Interactions

Natural and synthetic auxins, alone or combined with 50 μ M protodioscin, induced a significant primary root length reduction accompanied by an increase in number and length of lateral roots, compared to the control (Figure 3).

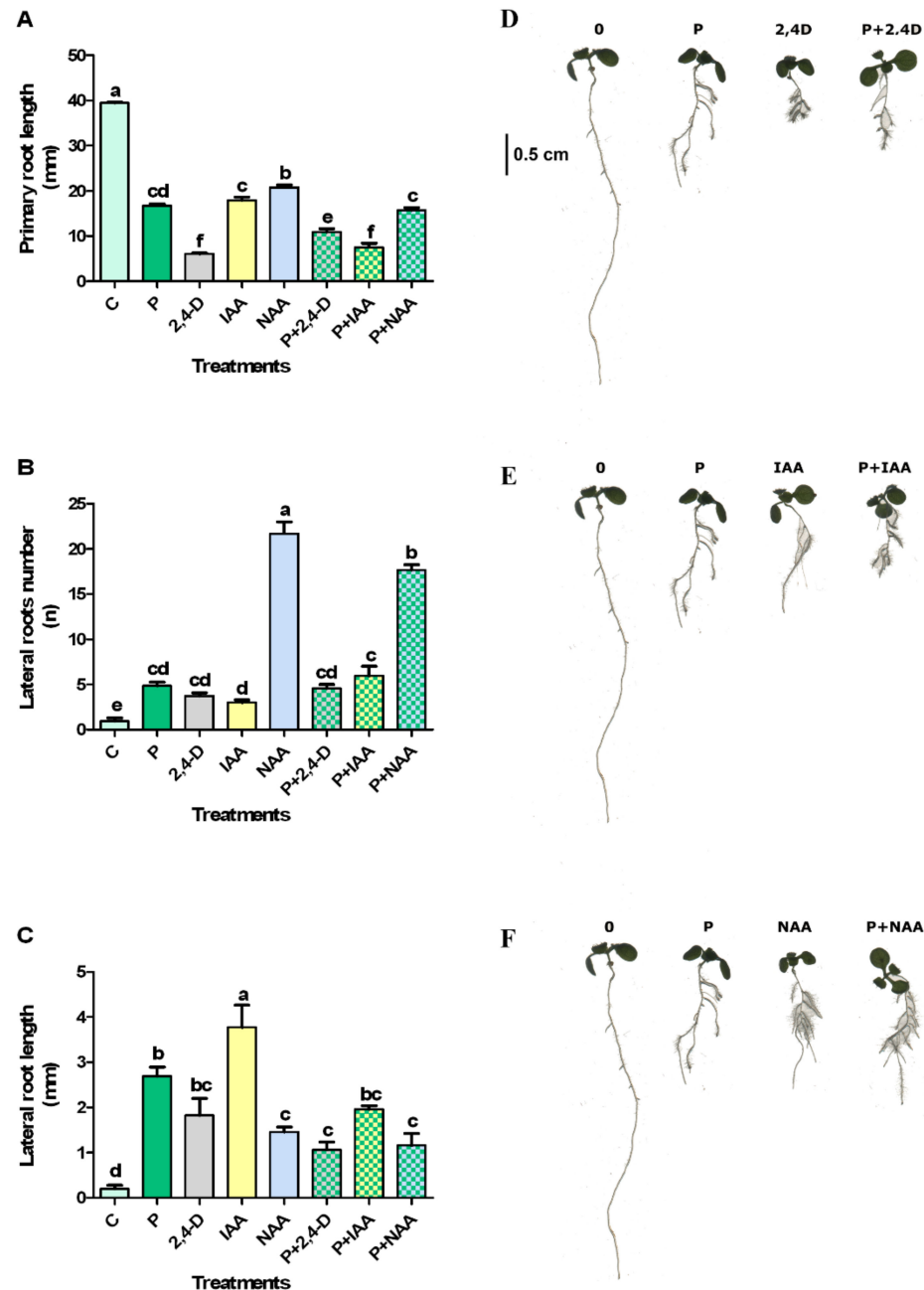


Figure 3. Primary root length (A,D), lateral roots number (B,E), and lateral root length (C,F) of *Arabidopsis* seedlings exposed to protodioscin (P) alone or in combination with auxins 2,4-D, IAA, and NAA (averaged data on the left side and representative image on the right side). Different letters indicate significant differences observed among treatments at $p \leq 0.05$ (SNK's test). $N = 4$.

In particular, 2,4-D alone caused the highest inhibition on primary root length, but this negative effect was reduced in combination with protodioscin. By contrast, IAA and NAA combined with protodioscin increased their inhibitory effect, further reducing primary root growth (Figure 3A,D).

All the treatments significantly increased the number of lateral roots compared to the control (Figure 3B,E). In particular, NAA alone or in combination with protodioscin was the most effective treatment in stimulating the lateral root number. An additive effect was observed with IAA and protodioscin treatment. Contrastingly, no significant differences were observed between 2,4-D alone or in combination with protodioscin (Figure 3B,E).

Finally, protodioscin and IAA, alone or combined, were the most effective treatments in stimulating the lateral root length. Conversely, 2,4-D and NAA alone or in combination with protodioscin did not show any differences (Figure 3C). The images of *Arabidopsis* treated seedlings confirmed these results (Figure 3D,F).

2.3. Effects of Protodioscin and Auxin Inhibitors

Since the root morphological changes are generally related to an altered auxin distribution and/or accumulation, the effect of auxin transport inhibitors (TIBA and NPA) and auxin antagonists (PCIB), alone or in combination with protodioscin, was analyzed. The results showed that PCIB, TIBA and NPA, alone or in combination with protodioscin, strongly inhibited the primary root length (Figure 4A). Furthermore, in primary root, TIBA and PCIB treatments induced a circumnating phenomenon typical of several transport and biosynthetic auxin inhibitors. Interestingly, this effect disappeared in combination with protodioscin, restoring the gravitropic root response (Figure 4D).

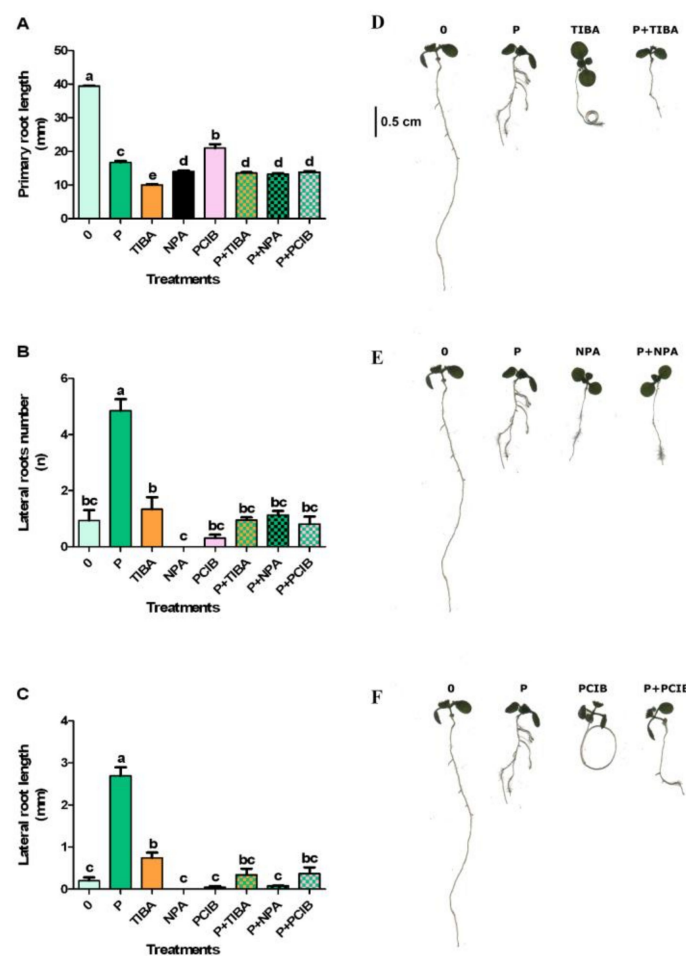


Figure 4. Primary root length (A,D), lateral roots number (B,E), and lateral root length (C,F) of *A. thaliana* seedlings treated with protodioscin (P), alone or in combination with auxin inhibitors TIBA, NPA, and PCIB (averaged data on the left side and representative image on the right side). Different letters indicate significant differences observed among treatments at $p \leq 0.05$ (SNK's test). N = 4.

All the other treatments did not cause any significant effect, except for protodioscin, which significantly stimulated the lateral root number (Figure 4B,E).

Finally, the lateral root length was significantly stimulated only by protodioscin and, at a lower extent, by TIBA (Figure 4C,F).

2.4. Auxin Distribution through Auxin-Responsive Reporter *pDR5::GFP* and Its Relative Quantification

The dose-response curves and the pharmacological approach suggested that protodioscin caused strong root development and growth alterations, probably mediated by an alteration of auxin concentration and/or distribution. The *Arabidopsis* transgenic line for the auxin-responsive reporter *pDR5::GFP* was used to validate this hypothesis, and the auxin content was quantified.

The *pDR5::GFP* transgenic line treated with protodioscin showed an evident impaired auxin distribution (Figure 5), displaying a maximum distribution in the quiescent center (QC) and initial columella cells, without extending to mature columella cells (Figure 5A'). Conversely, the control *pDR5::GFP* roots exhibited the typical auxin maximum distribution in the root tip (i.e., QC, initial and mature columella cells) (Figure 5A). Furthermore, treated *pDR5::GFP* roots displayed a stronger fluorescence signal locally in the elongation zone, specifically in xylem pole cells adjacent to the pericycle (Figure 5B), suggesting a potential auxin accumulation (Figure 5B').

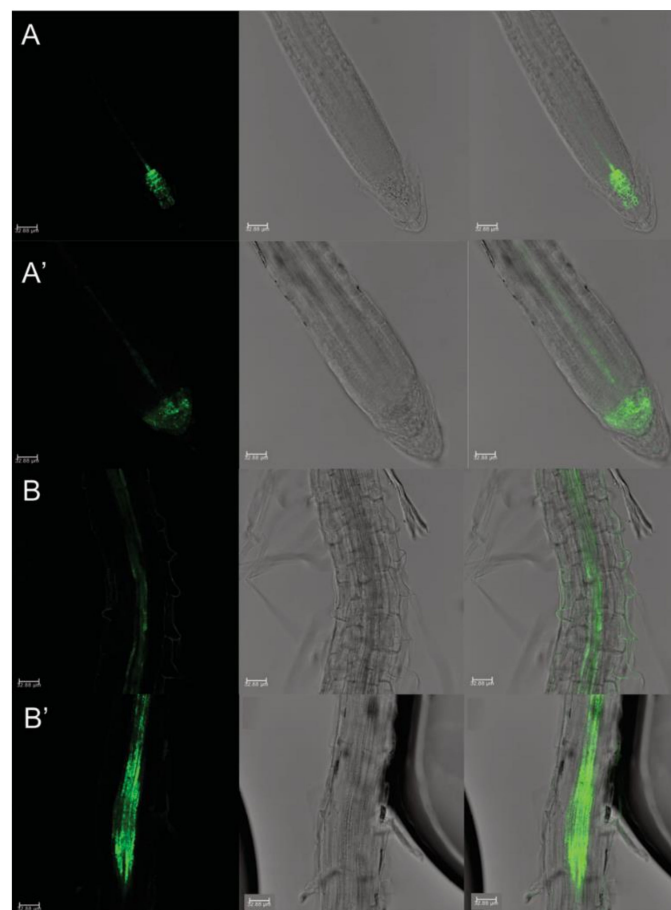


Figure 5. Primary root apex in seedlings of *Arabidopsis pDR5::GFP* transgenic line untreated (A) and treated with 50 μ M protodioscin for 6 d (A'). Root maturation zone of *A. thaliana pDR5::GFP* transgenic line untreated (B) and treated with 50 μ M protodioscin for 6 d (B'). Left side, GFP signal; center, transmission image; right side, merged image. Scale bars 32.88 μ m. N = 4.

This hypothesis was validated by the auxin quantification through GC-MS analysis, which pointed out a 21% accumulation of auxin higher than the control in mature root zone exposed to protodioscin (Figure 6).

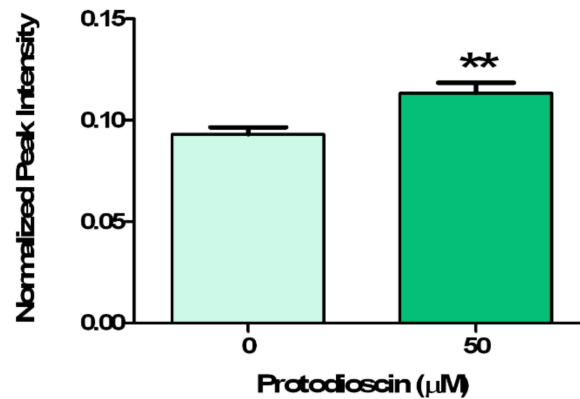


Figure 6. Relative quantification of IAA. Data are expressed as the average of the internal standard normalized intensity \pm SE. Statistical significance of the data was evaluated through a *t*-test with $p \leq 0.05$: * ($p \leq 0.05$), ** ($p \leq 0.01$), *** ($p \leq 0.001$). N = 3.

2.5. Protodioscin Affected Auxin Gradient and Polar Transport

The PINs: PINs-GFP transgenic lines were adopted to detect the different auxin transport proteins involved in the polar auxin gradient in protodioscin-treated and -untreated root apices (Figure 7).

The PIN1 resided at procambium and proendodermis cells, both in the meristem and distal elongation zone, in the untreated root apex (Figure 7A), while it was only revealed in a few cell layers of stele in the meristem zone in protodioscin-treated roots (Figure 7A'). The protodioscin treatment also affected the distribution pattern of PIN2 proteins, related to shootward/basipetal transport (Figure 7B,B'). In the control roots, the PIN2 proteins appeared at the apical side of the protodermis, at the lateral root cap cells, and mostly basally in the precortex cells, in the protodermis until the transition to the elongation zone (Figure 7B). Instead, protodioscin strongly altered the distribution of PIN2 proteins, whose signal was mainly localized in a bunch of proendodermal cells of the root meristem (Figure 7B'). The fluorescence signal was then diffused along the transition and elongation zone without a specific pattern, while no GFP signal was observed in the protodermis and precortex (Figure 7B').

The localization of PIN3 protein was also altered by treatment (Figure 7C,C'). In the untreated roots, PIN3 proteins are localized in tiers two and three of columella cells, at the basal side of vascular cells, and on the lateral side of the pericycle cells of the elongation zone (Figure 7C). Otherwise, in the protodioscin treated roots, PIN3 proteins are localized in the procambium cells of the distal elongation zone only (Figure 7C').

In the control, PIN4 and PIN7 proteins are mainly localized in provascular cells and all around the QC and surrounding cells, as well as in the provascular cells, meristem, and in the elongation zone, at the lateral and basal membranes (Figure 7D,E), respectively. They showed complete inhibition after protodioscin treatment in the root tips (Figure 7D',E').

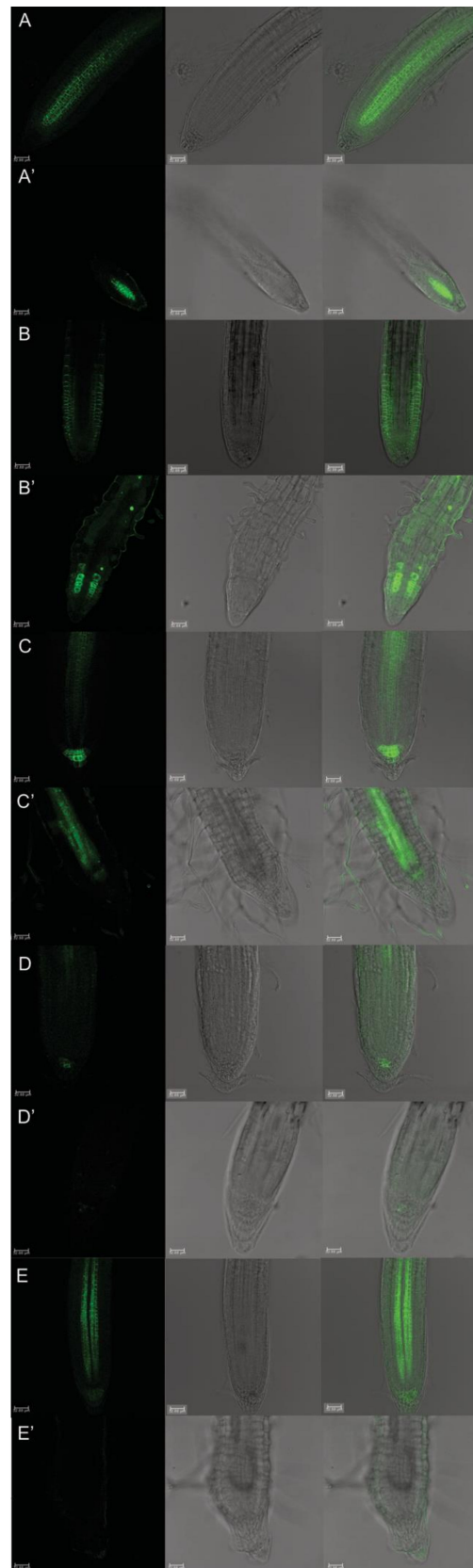


Figure 7. Primary root apex in seedlings of *Arabidopsis* *pPIN1::PIN1-GFP*, *pPIN2::PIN2-GFP*, *pPIN3::PIN3-GFP*, *pPIN4::PIN4-GFP*, *pPIN7::PIN7-GFP* transgenic lines untreated (**A–E**) and treated with 50 μ M protodioscin for 6 d (**A'–E'**). Scale bars 32.88 μ m. Left side, GFP signal; center, transmission image; right side, merged image. N = 4.

2.6. In Situ Semi-Quantitative Determination of H_2O_2 and O_2^-

Protodioscin (50 μ M) caused a H_2O_2 increase in roots of *A. thaliana*, compared to the control (Figure 8A,B), without changing the O_2^- production (Figure 8C,D).

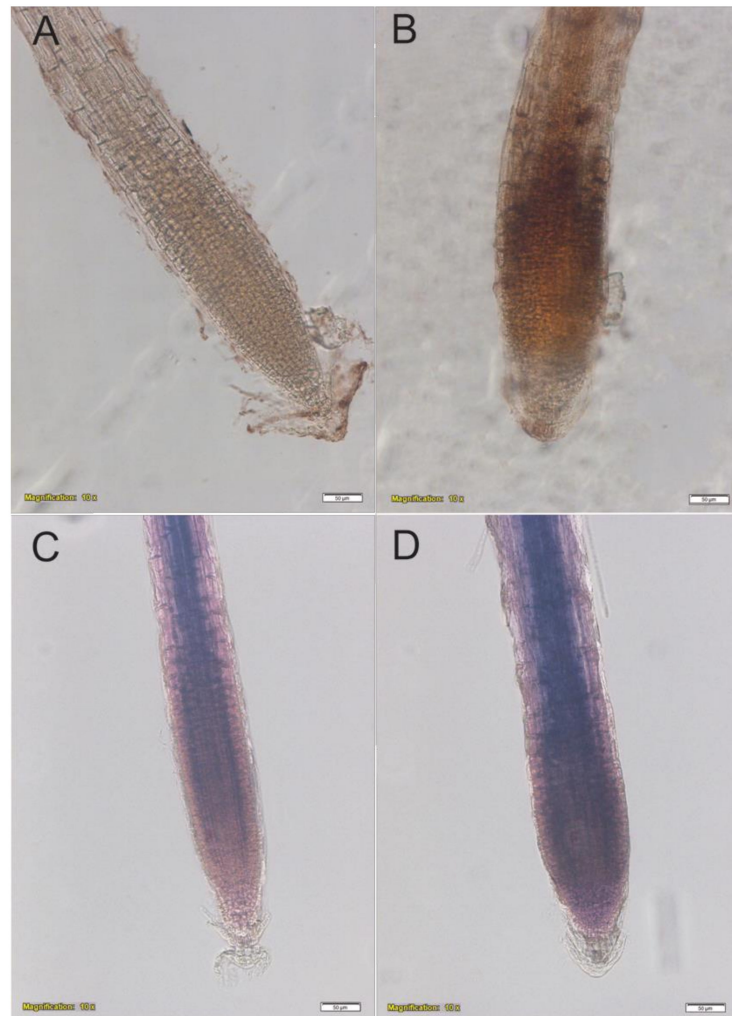


Figure 8. In situ hydrogen peroxide (dark brownish color) (A,B) and superoxide (dark blue color) (C,D) localization in roots of *A. thaliana* untreated (A,C) and treated with 50 μ M protodioscin for 6 d (B,D). Image magnification 10 \times , scale bar 50 μ m. N = 4.

3. Discussion

The in vitro assay revealed the inhibitory effects of protodioscin on *Arabidopsis* root growth, confirming the higher phytotoxic potential of this saponin [49–51], compared to other natural molecules [53]. The inhibition of primary root elongation was even observed at low concentrations, with an ED₅₀ equal to 50 μ M. A similar value was found in our previous study with the weed *I. grandifolia* (54 μ g mL⁻¹) and *D. insularis* (34 μ g mL⁻¹) [51]. An ED₅₀ of 240 μ M was found in *B. pilosa* by Mito et al., (2019). These values indicate that protodioscin has a higher inhibitory effect on weeds species when compared with the crop soybean. As reported by Nepomuceno et al. [49], protodioscin inhibits the root growth in soybean seedlings at a 680 μ M concentration. The ED₅₀ value (50 μ M) was then used for all the subsequent experiments to identify its mode of action.

Protodioscin reduced primary root growth in a dose-dependent manner, causing strong root deformation at the highest concentrations. This reduction was also accompanied by an increase in lateral root number and root hair density, which hinted at a correlation with auxin homeostasis [54]. Furthermore, the saponin caused a thickening of the root

apex, a phenomenon known as swelling, already observed with many natural compounds, such as coumarin [55,56], oryzalin [57], citral [58] and mainly attributable to an alteration of the cortical microtubules [59,60]. Similar results were also observed with the alkaloids narciclasine and norharmane [25,37], the sesquiterpene farnesene [26], which strongly affected microtubule organization and cellular ultrastructure of the meristematic apex in *Arabidopsis* roots, altering auxin transport and redistribution.

The root phenotype changes induced by protodioscin were associated with an increase in auxin content, underpinning that the protodioscin effect may be caused by the perturbation of auxin homeostasis. Similar effects were observed in *A. thaliana* seedlings exposed to phenylpropanoid 3,4-(methylenedioxy)cinnamic acid (MDCA) and benzoic acid [24,34].

Auxin plays an essential role in the root system by regulating cell division and differentiation in the meristematic and elongation zones. For example, it was proven that, under alkaline stress, the auxin accumulation in root tips negatively affected cell division in the meristem zone [61]. Recent studies pointed out that the auxin homeostasis perturbation led to allelochemical toxicity [61–63].

To provide an insight into the auxin–protodioscin interactions in *Arabidopsis* roots, natural and synthetic auxin, alone or in combination with the saponin, were added in the growth medium. The exogenous auxin applications did not ameliorate the inhibitory effects of protodioscin on primary root elongation; instead, it exacerbated the growth reduction, especially in combination with IAA or NAA, suggesting a negative additive interaction between them. Similar behaviour was observed with the lateral root number, which further increased in the presence of IAA or NAA and protodioscin. By contrast, the lateral root length was negatively affected by all the auxins co-supplied with protodioscin. Generally, in almost all the treatments, both the number and length of the lateral roots were still higher than the control.

Furthermore, the positive effect of saponin on the lateral root's number and length disappeared when the auxin transport inhibitors (TIBA and NPA) or the auxin antagonist (PCIB) were added, suggesting that protodioscin was not able to overcome their inhibitory effect on lateral root formation. Interestingly, the addition of protodioscin partially restored the gravitropic root responses generally observed in seedlings treated with TIBA and PCIB [64] characterized by a lateral root lack and root coils, typical of mutants with altered auxin transport and distribution. All these results strongly suggested the auxin-like activity of protodioscin.

Likewise, the auxin-like effect of non-auxin probe naxillin (reduction in primary root growth and stimulation of lateral root number) was due to an auxin distribution and stimulation of the conversion of the auxin precursor indole-3-butyric acid into the active auxin indole-3-acetic acid in the root cap [65]. According to our results, plants treated with naxillin showed an induction of the synthetic auxin-responsive marker *pDR5::GUS* in the xylem pole cells adjacent to the pericycle of the basal meristem, demonstrating the impairment of auxin distribution and suggesting auxin accumulation in the root area involved in lateral root development [65].

To explore whether protodioscin induced auxin accumulation affecting PAT, we examined the role of the major auxin polar carriers, using the *PINs::GFP* transgenic lines. PAT is mediated by auxin influx carriers, AUXIN1/LIKE AUXIN1 (AUX1/LAX) and auxin efflux proteins, PIN-FORMED (PIN) [66,67]. In *Arabidopsis*, there are eight PIN proteins (PIN1–PIN8) that regulate auxin homeostasis [68]. Among them, PIN1 mediates acropetal auxin transport in the root stele; PIN2 is required for the basipetal flow of auxin through outer root cell layers; PIN4 is expressed around the columella cells and localized toward the QC, contributing to the auxin concentration in this tissue; PIN3 and PIN7 are responsible for the outward and inward lateral transport of auxin in the root cap and mature root zone, respectively [65,69]. Many natural compounds regulate root growth by affecting auxin homeostasis and PINs expression. Narciclasine inhibits auxin transport in *Arabidopsis* by mainly affecting the subcellular trafficking of PIN and AUX1 proteins through interfering with actin cytoskeletal organization [37]. The sesquiterpene farnesene induced

auxin accumulation, mainly inhibiting PIN3 and PIN7 efflux carriers, which resulted in microtubule disorganization [70]. Recently, it was demonstrated that the allelochemical coumarin interferes with auxin polar transport, altering the microtubule cortical array organization and inducing, as in our experiments, root swelling and an increase in the lateral root number [60]. Furthermore, benzoic acid increased the auxin level in the root tips, associated with a higher expression of auxin biosynthesis and auxin polar transporter, AUX1 and PIN2 [24]. More recently, norharmine was shown to inhibit PIN2, PIN3 and PIN7 transport proteins, causing a significant inhibitory effect on the growth of *A. thaliana* seedlings [25].

Accordingly, protodioscin significantly interferes with all the PIN polar transporters, altering auxin distribution. The PINs::GFP imaged by confocal microscopy revealed a fall in the PIN4 and PIN7 GFP signal and an altered distribution in PIN1, PIN2 and PIN3 after protodioscin treatment. In further detail, PIN1 and PIN2 distribution were extremely reduced and localized only in the distal part of the root meristem, and PIN2 was only present on a few root meristem cells characterized by an abnormal shape. The alteration of the PIN1 proteins suggests a reduction in the downward movement of auxin (from the shoot to the root apex), although it was mediated by PIN3 proteins located in the stele region, which were less affected by the treatment. The modification induced by protodioscin of PIN2 could be responsible for a change in the root system plasticity as observed, especially under abiotic stress, such as aluminium and alkaline stress, which then inhibited primary root elongation by altering auxin distribution via disturbing the AUX1/PIN2-mediated auxin transport [60,71]. PIN3 was weakly expressed in the columella cells but highly accumulated in the stele. This distribution suggested a reduction in auxin in the QC and its accumulation in the elongation zone, as also observed using the auxin-inducible reporter *pDR5::GFP*. Furthermore, PIN4 and PIN7, which are involved in auxin lateral redistribution (PIN7) and downward distribution from the QC to the columella (PIN4) [65,67,72], respectively, were significantly altered at the QC and columella level, confirming an alteration of auxin distribution in the distal meristem and suggesting a potentially biased accumulation of auxin at the QC level.

Blilou et al. [66] reported that PIN1, PIN3 and PIN7 loss, combined with defective PIN2 induced a drastic reduction in primary root growth. These data might support the hypothesis that the alterations induced by protodioscin on PIN proteins might lead to the observed alterations in primary root development. Moreover, the accumulation in auxin observed in the xylem pole cells adjacent to the pericycle (*pDR5::GFP*) and the increase in fluorescence observed in PIN3 close to the elongation zone could suggest auxin accumulation (supported by the GC-MS) in the root pericycle, where lateral root initiation occurs. This could justify the protodioscin-induced increase in lateral root number observed in our experiments. Indeed, it is well known that auxin response maximally promotes a subset of xylem pole-associated pericycle cells to provide the competence to form lateral roots [73–76].

Root morphology changes, plant hormonal alterations, microtubule disorganization induced by phytotoxin generally caused higher ROS production [77,78]. ROS-induced oxidative damage is widely considered to be associated with allelopathic toxicity [17,79,80]. The gallic acid was reported to trigger high ROS levels in roots, leading to microtubule disruption and root architecture collapse [79]. Likewise, benzoic acid increased ROS levels in the meristematic, elongation, and mature root regions of *Arabidopsis* [24]. In our study, plants treated with protodioscin in situ stained for H₂O₂ confirmed the increased accumulation in roots. This result is in agreement with our previous work showing an increased content of ROS in *I. grandifolia* and *D. insularis* roots treated with protodioscin [51]. Furthermore, this increase was also recently observed in roots exposed to nerolidol [20] and benzoic acid [24] and was accompanied by root morphological alterations.

4. Materials and Methods

4.1. Plant Material and Experimental Design

A. thaliana, ecotype Columbia (Col-0) seeds were sterilized and vernalized, as reported by Araniti et al. [70]. They were sown and then germinated on square Petri dishes (100 × 100 mm) containing agar (0.8% agar *w/v*) enriched with a mixture of micro- and macronutrients (Murashige-Skoog, Sigma-Aldrich SRL, Milan, Italy) and supplemented with 1% sucrose (*w/w*). The Petri dishes were then placed vertically in a growth chamber at 22 ± 1 °C and $120 \mu\text{mol m}^{-2} \text{s}^{-1}$ light intensity provided by a cold white fluorescent lamp (Polylux XL FT8, 55 W 8440, Barcelona, Spain), for a photoperiod of 8/16 h light/dark, and 55% relative humidity. After germination, five seedlings (4 days old) for each replicate were transferred to a single Petri dish containing the aforementioned medium supplemented with 0, 15.6, 31.3, 62.5, 125, 250, and 500 μM protodioscin (P) concentrations for 6 d and placed in the growth chamber under the same conditions described above. Protodioscin (Aktin chemicals Inc., Chengdu, China) was diluted in the medium by autoclaving. After 6 d of treatment, the primary root length was measured, and the average growth was calculated. These values allowed us to determine the ED₅₀ value (dose causing 50% inhibition of the total response) used for all the subsequent experiments. The roots image was captured by scanning (STD 1600, Régent Instruments Inc., QC, Canada), and the primary and lateral root lengths (PRL and LRL, respectively) were measured using Image-Pro Plus v 6.0 software (Meia Cybernetics). The lateral root number was counted manually from the image (Abenavoli et al., 2008). The root hair length (RHL), density (RHD) (determined as the number of hairs in each of the apical segments (1 mm) of root observed), and apex width (AW) were determined by using stereoscopic microscopy (Olympus SZX9, Shinjuku, Tokyo, Japan) and Image-Pro Plus v 6.0 software (Meia Cybernetics, Rockville, USA).

4.2. Protodioscin and Auxins Interaction in Roots of *A. thaliana*

To determine the role of auxin on the protodioscin impact on the root system, a pharmacological approach was followed. In particular, the natural/synthetic auxins (2,4-dichlorophenoxyacetic acid (2,4-D), indole-3-acetic acid (IAA) and α -naphthalen acetic acid (NAA)), transport inhibitors (2,3,5-triiodobenzoic acid (TIBA) and N-1-naphthylphthalamic acid (NPA)) and an anti-auxin (p-chlorophenoxyisobutyric acid (PCIB)) were applied alone or in combination with protodioscin (50 μM) during *Arabidopsis* seedling growth. Seedlings were grown as previously described for 4 d and then transferred on an agarized medium enriched with mineral nutrients and the abovementioned compounds (Table 1).

Table 1. Concentrations of natural/synthetic auxins, transport inhibitor, anti-auxin and/or protodioscin (P) used in the interaction assay.

Molecules	Concentrations μM
P	50
TIBA	15
NPA	5
PCIB	15
2,4-D	0.1
IAA	0.1
NAA	0.1
P + TIBA	50 + 15
P + NPA	50 + 5
P + PCIB	50 + 15
P + 2,4-D	50 + 0.1
P + IAA	50 + 0.1
P + NAA	50 + 0.1

4.3. *Arabidopsis* Transgenic Reporter Lines Bioassay

Seeds of *Arabidopsis* transgenic lines (background Columbia 0), and in particular, the synthetic reporter *pDR5::GFP*, and different auxin transport proteins *pPIN1::PIN1-GFP*, *pPIN2::PIN2-GFP*, *pPIN3::PIN3-GFP*, *pPIN4::PIN4-GFP*, and *pPIN7::PIN7-GFP*, were germinated and grown as previously reported. Five seedlings (4 d old) were then transferred to a single Petri dish containing the same medium previously described and enriched with 50 μM protodioscin for each treatment and replicate ($N = 6$). The transplanted seedlings were then placed in a growth chamber for 6 d and grown as previously described.

The *Arabidopsis* roots were then collected, fixed for 1 min in 4% (*w/v*) paraformaldehyde in 1X Phosphate Buffer Saline (PBS) (pH 7.0) and mounted in a 1:1 solution of glycerol: PBS (1X). Confocal images of median longitudinal sections were acquired using a Leica inverted TCS SP8 confocal scanning laser microscope, with a 40 \times oil immersion objective. The detection of Green Fluorescent Protein (GFP) (excitation peak centered at about 488 nm, an emission peak wavelength of 509 nm) was performed by combining the settings indicated in the microscope's sequential scanning facility. More than 20 seedlings were analyzed per treatment, and four independent experiments were carried out.

4.4. *In Situ* Semi-Quantitative Determination of H_2O_2 and O_2^-

Treated (P 50 μM) and untreated root tips (control) were cut, immediately immersed in distilled water, and vacuum infiltrated for 5 min with 0.65 mg mL^{-1} sodium azide solution (NaN_3) in potassium phosphate buffer (pH 7.8) containing 0.1% (*w/v*) nitroblue tetrazolium (NBT), for O_2^- detection.

For *in situ* H_2O_2 localization, treated and untreated root tips were transferred in acidified water (pH 3.8) containing 3,3'-diaminobenzidine (DAB) (1 mg mL^{-1}) and infiltrated in vacuum conditions for 5 min.

After infiltration, the roots were incubated in darkness for 20 min in the same buffer and then illuminated until the stains appeared: reddish-brown or dark blue colour, for DAB or NBT, respectively [26]. The stained areas were determined by image analysis with the software Image ProPlus v.6.0 (Media Cybernetics Inc., Bethesda, MD, USA).

4.5. IAA Relative Quantification through GC-MS Analysis

Indole-3-acetic acid (IAA) quantification was carried out following the method proposed by Rawlinson et al. [81] with some modifications.

At the end of the protodioscin treatment, the *Arabidopsis* roots were snap-frozen in liquid nitrogen, powdered, and sorted in 2 mL vials, using 100 mg of plant material for each treatment and replicate. For sample normalization and IAA relative quantification, 20 μL of 3-indolepropionic acid (IPA) (20 mg $\cdot\text{mL}^{-1}$) were added as an internal standard.

For IAA extraction, 200 μL of NaOH (1% *w/v*), 147 μL of methanol (MeOH), and 34 μL of pyridine were added, and the samples were vortexed for 40 s. IAA derivatization was achieved by adding to the extracted samples 20 μL of methyl chloroformate and vortexing for 30 s (the step was repeated twice).

To the derivatized extract, 400 μL of chloroform and 400 μL of NaHCO_3 solution (50 mM stock) were added; the samples were vigorously vortexed for 20 s and then centrifuged at 14,000 rpm for 1 min to allow organic/inorganic layers separation. The organic lower phase was collected and dispensed into a new 2 mL centrifuge tube, and the aqueous residues were eliminated, using anhydrous Na_2SO_4 . An aliquot (100 μL) of this organic phase was used for gas chromatography-mass spectrometry (GC-MS) analysis. A parallel experiment was carried out using pure IAA (Sigma Aldrich, 20149, Milano, Italy, Cat. No. I3750-25G-A) as an external standard for retention time (RT) assignment.

The GC-MS analysis was carried out using a Thermo Fisher gas chromatography apparatus (Trace 1310) equipped with a single quadrupole mass spectrometer (ISQ LT). The capillary column (MEGA -5MS, 30 m \times 0.25 mm \times 0.25 μm + 10 m of pre-column) (MEGA S.r.l., Legnano (MI), Italy) and the gas carrier was helium with a flow rate of 1 $\text{mL}\cdot\text{min}^{-1}$. The injector and transfer lines were settled at 250 $^\circ\text{C}$ and 270 $^\circ\text{C}$, respectively. A total of

3 µL of the sample was injected with a 35 psi pressure pulse, held for 1 min. The following temperature was programmed: isocratic for 1 min at 40 °C, from 40 °C to 320 °C with a rate of 20 °C × min, then isocratic for 2 min 320 °C. The ion source was settled at 200 °C, and the solvent delay was 4.5 min. Mass spectra were recorded in electronic impact (EI) mode at 70 eV, scanning at 50–400 m/z range. Then the MS was run in selected ion monitoring (SIM), using one quantifier ion (189 m/z) and two qualifiers (103 and 77 m/z) for IAA-Me ester identification. A mixture of alkanes was injected at the beginning of the experiment (C10-C40 all even) for retention index calculation. Finally, peak identification was carried out with the help of the commercial library (NIST 2011). The data were then expressed as a normalized (on an internal standard basis) peak intensity.

4.6. Statistical Analysis

All the experiments were carried out in a completely randomized design, with N = 4 for dose-response curves, N = 4 for pharmacological bioassay, and N = 3 for IAA quantification.

The dose-response curves data and pharmacological bioassay were expressed as mean ± standard errors (SE), and the data were analyzed using analysis of variance (ANOVA) with SNK's test, post-hoc ($p \leq 0.05$). Differences in auxin content were evaluated using the *t*-test ($p \leq 0.05$).

The ED₅₀ parameter was calculated, tightening the dose-response curve's raw data through a non-linear regression log–logistic equation model. The equation was chosen from those that had the highest determination coefficient (r^2) (best fit) (Software Graph-Pad Prism).

5. Conclusions

Our results provide an explanation for the molecular mechanisms underlying the effects of protodioscin on root growth. This molecule alters the hormonal balance, inducing auxin accumulation, and stimulates oxidative damage through the production of H₂O₂.

ROS production may alter the normal root growth, interfering with cell division and cytokinesis and consequently inducing root morphology alterations. The auxin accumulation could be the main reason for the increase in the number of lateral roots observed. Based on our results, we conclude that the saponin protodioscin is able to modulate the root system of *A. thaliana* by interfering with the auxin transport (PAT) and signalling.

Author Contributions: Conceptualization, M.R.A., E.L.I.-I., F.A.; methodology, M.R.A., F.A., L.B.; software, A.L.S.W., F.A., L.B.; validation, A.L.S.W.; formal analysis, A.L.S.W., L.B., F.A.; investigation, A.L.S.W.; resources, M.R.A., E.L.I.-I., F.A.; data curation, A.L.S.W., F.A.; writing and original draft preparation, A.L.S.W., M.R.A., E.L.I.-I., F.A.; writing-review and editing, A.L.S.W., M.R.A., E.L.I.-I., F.A., L.B.; visualization, A.L.S.W., M.R.A., E.L.I.-I., F.A., L.B.; supervision, M.R.A., E.L.I.-I., F.A.; project administration, M.R.A., E.L.I.-I., F.A.; funding responsible, E.L.I.-I. All authors have read and agreed to the published version of the manuscript.

Funding: This work was supported by grants from the Araucária Foundation (112/2010) do Estado do Paraná, National Council for Scientific and Technological Development (CNPq). Ana Luiza Wagner Zampieri is a fellowship holder from the coordination for the Improvement of Higher Education Personnel (CAPES).

Acknowledgments: We would like to say thanks to Jiri Friml, Hyung-Taeg Cho, Ikram Blilou, Marcus Heisler, who provided the mutated lines used in the experiments.

Conflicts of Interest: The authors declare that they have no conflict of interest.

References

1. Chauhan, B.S. Grand challenges in weed management. *Front. Agron.* **2020**, *1*, 3. [[CrossRef](#)]
2. Monaco, T.J.; Weller, S.C.; Ashton, F.M. *Weed Science: Principles and Practices*; John Wiley & Sons: Hoboken, NJ, USA, 2002.
3. Clapp, J. Explaining growing glyphosate use: The political economy of herbicide-dependent agriculture. *Glob. Environ. Chang.* **2021**, *67*, 102239. [[CrossRef](#)]

4. Rosculete, C.A.; Bonciu, E.; Rosculete, E.; Olaru, L.A. Determination of the environmental pollution potential of some herbicides by the assessment of cytotoxic and genotoxic effects on *Allium cepa*. *Int. J. Environ. Res. Public Health* **2019**, *16*, 75. [[CrossRef](#)]
5. Heap, I. International Herbicide-Resistant Weed Database. 2019. Available online: www.weedscience.org (accessed on 26 February 2020).
6. Al-Samarai, G.F.; Mahdi, W.M.; Al-Hilali, B.M. Reducing environmental pollution by chemical herbicides using natural plant derivatives—Allelopathy effect. *Ann. Agric. Environ. Med.* **2018**, *25*, 449–452. [[CrossRef](#)] [[PubMed](#)]
7. Verdeguer, M.; Sánchez-Moreiras, A.M.; Araniti, F. Phytotoxic effects and mechanism of action of essential oils and terpenoids. *Plants* **2020**, *9*, 1571. [[CrossRef](#)] [[PubMed](#)]
8. Dayan, F.E. Is there a natural route to the next generation of herbicides? *Outlooks Pest Manag.* **2018**, *29*, 54–57. [[CrossRef](#)]
9. Dayan, F.E. Current status and future prospects in herbicide discovery. *Plants* **2019**, *8*, 341. [[CrossRef](#)] [[PubMed](#)]
10. Araniti, F.; Mancuso, R.; Lupini, A.; Giofrè, S.V.; Sunseri, F.; Gabriele, B.; Abenavoli, M.R. Phytotoxic potential and biological activity of three synthetic coumarin derivatives as new natural-like herbicides. *Molecules* **2015**, *20*, 17883–17902. [[CrossRef](#)]
11. Araniti, F.; Mancuso, R.; Lupini, A.; Sunseri, F.; Abenavoli, M.R.; Gabriele, B. Benzofuran-2-acetic esters as a new class of natural-like herbicides. *Pest Manag. Sci.* **2020**, *76*, 395–404. [[CrossRef](#)]
12. Dayan, F.E.; Duke, S.O. Natural compounds as next-generation herbicides. *Plant Physiol.* **2014**, *166*, 1090–1105. [[CrossRef](#)]
13. Aşkin Çelik, T.; Aslantürk, Ö.S. Evaluation of cytotoxicity and genotoxicity of *Inula viscosa* leaf extracts with *Allium test*. *J. Biomed. Biotechnol.* **2010**, *2010*, 189252. [[CrossRef](#)] [[PubMed](#)]
14. Lupini, A.; Araniti, F.; Mauceri, A.; Princi, M.; Sorgonà, A.; Sunseri, F.; Varanini, Z.; Abenavoli, M. Coumarin enhances nitrate uptake in maize roots through modulation of plasma membrane H⁺-ATPase activity. *Plant Biol.* **2018**, *20*, 390–398. [[CrossRef](#)]
15. Scavo, A.; Abbate, C.; Mauromicale, G. Plant allelochemicals: Agronomic, nutritional and ecological relevance in the soil system. *Plant Soil* **2019**, *442*, 23–48. [[CrossRef](#)]
16. Araniti, F.; Landi, M.; Lupini, A.; Sunseri, F.; Guidi, L.; Abenavoli, M. *Origanum vulgare* essential oils inhibit glutamate and aspartate metabolism altering the photorespiratory pathway in *Arabidopsis thaliana* seedlings. *J. Plant Physiol.* **2018**, *231*, 297–309. [[CrossRef](#)] [[PubMed](#)]
17. Araniti, F.; Miras-Moreno, B.; Lucini, L.; Landi, M.; Abenavoli, M.R. Metabolomic, proteomic and physiological insights into the potential mode of action of thymol, a phytotoxic natural monoterpene phenol. *Plant Physiol. Biochem.* **2020**, *153*, 141–153. [[CrossRef](#)] [[PubMed](#)]
18. Sánchez-Moreiras, A.M.; Graña, E.; Reigosa, M.J.; Araniti, F. Imaging of chlorophyll a fluorescence in natural compound-induced stress detection. *Front. Plant Sci.* **2020**, *11*, 1991. [[CrossRef](#)] [[PubMed](#)]
19. Ishii-Iwamoto, E.; Abraham, D.; Sert, M.; Bonato, C.; Kelmer-Bracht, A.; Bracht, A. Mitochondria as a site of allelochemical action. In *Allelopathy*; Springer: Berlin/Heidelberg, Germany, 2006; pp. 267–284.
20. Landi, M.; Misra, B.B.; Muto, A.; Bruno, L.; Araniti, F. Phytotoxicity, morphological, and metabolic effects of the sesquiterpene nerolidol on *Arabidopsis thaliana* seedling roots. *Plants* **2020**, *9*, 1347. [[CrossRef](#)]
21. Na, X.; Hu, Y.; Yue, K.; Lu, H.; Jia, P.; Wang, H.; Wang, X.; Bi, Y. Narciclasine modulates polar auxin transport in *Arabidopsis* roots. *J. Plant Physiol.* **2011**, *168*, 1149–1156. [[CrossRef](#)] [[PubMed](#)]
22. Céspedes, C.L.; Marín, J.C.; Domínguez, M.; Avila, J.G.; Serrato, B. Plant growth inhibitory activities by secondary metabolites isolated from Latin American flora. *Adv. Phytomed.* **2006**, *2*, 373–410.
23. Lotina-Hennsen, B.; King-Diaz, B.; Aguilar, M.; Terrones, M.H. Plant secondary metabolites. Targets and mechanisms of allelopathy. In *Allelopathy*; Springer: Berlin/Heidelberg, Germany, 2006; pp. 229–265.
24. Zhang, W.; Lu, L.-Y.; Hu, L.-Y.; Cao, W.; Sun, K.; Sun, Q.-B.; Siddique, A.; Shi, R.-H.; Dai, C.-C. Evidence for the involvement of auxin, ethylene and ROS signaling during primary root inhibition of *Arabidopsis* by the allelochemical benzoic acid. *Plant Cell Physiol.* **2018**, *59*, 1889–1904. [[CrossRef](#)] [[PubMed](#)]
25. López-González, D.; Costas-Gil, A.; Reigosa, M.J.; Araniti, F.; Sánchez-Moreiras, A.M. A natural indole alkaloid, norharmane, affects PIN expression patterns and compromises root growth in *Arabidopsis thaliana*. *Plant Physiol. Biochem.* **2020**, *151*, 378–390. [[CrossRef](#)]
26. Araniti, F.; Grana, E.; Krasuska, U.; Bogatek, R.; Reigosa, M.J.; Abenavoli, M.R.; Sanchez-Moreiras, A.M. Loss of gravitropism in farnesene-treated *Arabidopsis* is due to microtubule malformations related to hormonal and ROS unbalance. *PLoS ONE* **2016**, *11*, e0160202. [[CrossRef](#)] [[PubMed](#)]
27. Lupini, A.; Araniti, F.; Sunseri, F.; Abenavoli, M.R. Coumarin interacts with auxin polar transport to modify root system architecture in *Arabidopsis thaliana*. *Plant Growth Regul.* **2014**, *74*, 23–31. [[CrossRef](#)]
28. Graña, E.; Sotelo, T.; Díaz-Tielas, C.; Araniti, F.; Krasuska, U.; Bogatek, R.; Reigosa, M.J.; Sánchez-Moreiras, A.M. Citral induces auxin and ethylene-mediated malformations and arrests cell division in *Arabidopsis thaliana* roots. *J. Chem. Ecol.* **2013**, *39*, 271–282. [[CrossRef](#)]
29. Wu, J.; Long, J.; Lin, X.; Chang, Z.; Baerson, S.R.; Ding, C.; Wu, X.; Pan, Z.; Song, Y.; Zeng, R. Momilactone B inhibits *Arabidopsis* growth and development via disruption of ABA and auxin signaling. *bioRxiv* **2020**. [[CrossRef](#)]
30. Teale, W.D.; Paponov, I.A.; Palme, K. Auxin in action: Signalling, transport and the control of plant growth and development. *Nat. Rev. Mol. Cell Biol.* **2006**, *7*, 847–859. [[CrossRef](#)]
31. Kleine-Vehn, J.; Ding, Z.; Jones, A.R.; Tasaka, M.; Morita, M.T.; Friml, J. Gravity-induced PIN transcytosis for polarization of auxin fluxes in gravity-sensing root cells. *Proc. Natl. Acad. Sci. USA* **2010**, *107*, 22344–22349. [[CrossRef](#)] [[PubMed](#)]

32. Im Kim, J.; Sharkhuu, A.; Jin, J.B.; Li, P.; Jeong, J.C.; Baek, D.; Lee, S.Y.; Blakeslee, J.J.; Murphy, A.S.; Bohnert, H.J. yucca6, a dominant mutation in Arabidopsis, affects auxin accumulation and auxin-related phenotypes. *Plant Physiol.* **2007**, *145*, 722–735. [[CrossRef](#)]
33. Sauer, M.; Balla, J.; Luschnig, C.; Wiśniewska, J.; Reinöhl, V.; Friml, J.; Benková, E. Canalization of auxin flow by Aux/IAA-ARF-dependent feedback regulation of PIN polarity. *Genes Dev.* **2006**, *20*, 2902–2911. [[CrossRef](#)]
34. Steenackers, W.; Cesarino, I.; Klíma, P.; Quareshy, M.; Vanholme, R.; Corneillie, S.; Kumpf, R.P.; Van de Wouwer, D.; Ljung, K.; Goeminne, G. The allelochemical MDCA inhibits lignification and affects auxin homeostasis. *Plant Physiol.* **2016**, *172*, 874–888. [[CrossRef](#)]
35. Li, X.; Gruber, M.Y.; Hegedus, D.D.; Lydiate, D.J.; Gao, M.-J. Effects of a coumarin derivative, 4-methylumbelliferone, on seed germination and seedling establishment in Arabidopsis. *J. Chem. Ecol.* **2011**, *37*, 880. [[CrossRef](#)] [[PubMed](#)]
36. Graña, E.; Costas-Gil, A.; Longueira, S.; Celeiro, M.; Teijeira, M.; Reigosa, M.J.; Sánchez-Moreiras, A.M. Auxin-like effects of the natural coumarin scopoletin on Arabidopsis cell structure and morphology. *J. Plant Physiol.* **2017**, *218*, 45–55. [[CrossRef](#)] [[PubMed](#)]
37. Hu, Y.; Na, X.; Li, J.; Yang, L.; You, J.; Liang, X.; Wang, J.; Peng, L.; Bi, Y. Narciclasine, a potential allelochemical, affects subcellular trafficking of auxin transporter proteins and actin cytoskeleton dynamics in Arabidopsis roots. *Planta* **2015**, *242*, 1349–1360. [[CrossRef](#)] [[PubMed](#)]
38. Hu, Y.; Yang, L.; Na, X.; You, J.; Hu, W.; Liang, X.; Liu, J.; Mao, L.; Wang, X.; Wang, H. Narciclasine inhibits the responses of Arabidopsis roots to auxin. *Planta* **2012**, *236*, 597–612. [[CrossRef](#)]
39. Jones, D.; Blancaflor, E.; Kochian, L.; Gilroy, S. Spatial coordination of aluminium uptake, production of reactive oxygen species, callose production and wall rigidification in maize roots. *Plant Cell Environ.* **2006**, *29*, 1309–1318. [[CrossRef](#)]
40. Zhang, P.; Luo, Q.; Wang, R.; Xu, J. Hydrogen sulfide toxicity inhibits primary root growth through the ROS-NO pathway. *Sci. Rep.* **2017**, *7*, 868. [[CrossRef](#)]
41. Dunand, C.; Crèvecoeur, M.; Penel, C. Distribution of superoxide and hydrogen peroxide in Arabidopsis root and their influence on root development: Possible interaction with peroxidases. *New Phytol.* **2007**, *174*, 332–341. [[CrossRef](#)]
42. Romero-Puertas, M.; Rodríguez-Serrano, M.; Corpas, F.; Gomez, M.D.; Del Rio, L.; Sandalio, L. Cadmium-induced subcellular accumulation of $O_2^{\cdot-}$ and H_2O_2 in pea leaves. *Plant Cell Environ.* **2004**, *27*, 1122–1134. [[CrossRef](#)]
43. Liu, G.; Gao, S.; Tian, H.; Wu, W.; Robert, H.S.; Ding, Z. Local transcriptional control of YUCCA regulates auxin promoted root-growth inhibition in response to aluminium stress in Arabidopsis. *PLoS Genet.* **2016**, *12*, e1006360. [[CrossRef](#)] [[PubMed](#)]
44. Gauthaman, K.; Ganesan, A.P.; Prasad, R. Sexual effects of puncturevine (*Tribulus terrestris*) extract (protodioscin): An evaluation using a rat model. *J. Altern. Complementary Med.* **2003**, *9*, 257–265. [[CrossRef](#)] [[PubMed](#)]
45. Leal, E.S.; Ítavo, L.C.V.; do Valle, C.B.; Ítavo, C.C.B.F.; Dias, A.M.; dos Santos Difante, G.; Barbosa-Ferreira, M.; Nonato, L.M.; de Melo, G.K.A.; Gurgel, A.L.C. Influence of protodioscin content on digestibility and in vitro degradation kinetics in *Urochloa brizantha* cultivars. *Crop Pasture Sci.* **2020**, *71*, 278–284. [[CrossRef](#)]
46. Sao Miguel, A.; Pacheco, L.; Souza, E.; Silva, C.; Carvalho, I. Cover crops in the weed management in soybean culture. *Planta Daninha* **2018**, *36*. [[CrossRef](#)]
47. Oliveira, R., Jr.; Rios, F.; Constantin, J.; Ishii-Iwamoto, E.; Gemelli, A.; Martini, P. Grass straw mulching to suppress emergence and early growth of weeds. *Planta Daninha* **2014**, *32*, 11–17. [[CrossRef](#)]
48. Silva, A. Isolamento e identificação de aleloquímicos de diversas espécies de plantas com potencial herbicida. *Dissertation Univ. Mar. Braz.* **2012**, *115*.
49. Nepomuceno, M.; Chinchilla, N.; Varela, R.M.; Molinillo, J.M.; Lacrete, R.; Alves, P.L.; Macias, F.A. Chemical evidence for the effect of *Urochloa ruziziensis* on glyphosate-resistant soybeans. *Pest Manag. Sci.* **2017**, *73*, 2071–2078. [[CrossRef](#)]
50. Mito, M.; Silva, A.; Kagami, F.; Almeida, J.; Mantovanelli, G.; Barbosa, M.; Kern-Cardoso, K.; Ishii-Iwamoto, E. Responses of the weed *Bidens pilosa* L. to exogenous application of the steroidal saponin protodioscin and plant growth regulators 24-epibrassinolide, indol-3-acetic acid and abscisic acid. *Plant Biol.* **2019**, *21*, 326–335.
51. Menezes, P.V.M.C.; Silva, A.A.; Mito, M.S.; Mantovanelli, G.C.; Stulp, G.F.; Wagner, A.L.; Constantin, R.P.; Baldoqui, D.C.; Gonçalves Silva, R.; Oliveira do Carmo, A.A.; et al. Morphogenic responses and biochemical alterations induced by the cover crop *Urochloa ruziziensis* and its component protodioscin in weed species. *Plant Physiol. Biochem.* **2021**, *166*, 857–873. [[CrossRef](#)]
52. Pennacchio, M.; Jefferson, L.V.; Havens, K. *Arabidopsis thaliana*: A new test species for phytotoxic bioassays. *J. Chem. Ecol.* **2005**, *31*, 1877–1885. [[CrossRef](#)]
53. Reigosa, M.; Pazos-Malvido, E. Phytotoxic effects of 21 plant secondary metabolites on *Arabidopsis thaliana* germination and root growth. *J. Chem. Ecol.* **2007**, *33*, 1456–1466. [[CrossRef](#)]
54. Overvoorde, P.; Fukaki, H.; Beeckman, T. Auxin control of root development. *Cold Spring Harb. Perspect. Biol.* **2010**, *2*, a001537. [[CrossRef](#)]
55. Abenavoli, M.R.; Sorgonà, A.; Albano, S.; Cacco, G. Coumarin differentially affects the morphology of different root types of maize seedlings. *J. Chem. Ecol.* **2004**, *30*, 1871–1883. [[CrossRef](#)] [[PubMed](#)]
56. Lupini, A.; Sorgonà, A.; Miller, A.J.; Abenavoli, M.R. Short-term effects of coumarin along the maize primary root axis. *Plant Signal. Behav.* **2010**, *5*, 1395–1400. [[CrossRef](#)]

57. Baskin, T.I.; Beemster, G.T.; Judy-March, J.E.; Marga, F. Disorganization of cortical microtubules stimulates tangential expansion and reduces the uniformity of cellulose microfibril alignment among cells in the root of *Arabidopsis*. *Plant Physiol.* **2004**, *135*, 2279–2290. [[CrossRef](#)] [[PubMed](#)]
58. Chaimovitsh, D.; Abu-Abied, M.; Belausov, E.; Rubin, B.; Dudai, N.; Sadot, E. Microtubules are an intracellular target of the plant terpene citral. *Plant J.* **2010**, *61*, 399–408. [[CrossRef](#)]
59. Häntzschel, K.; Weber, G. Blockage of mitosis in maize root tips using colchicine-alternatives. *Protoplasma* **2010**, *241*, 99–104. [[CrossRef](#)] [[PubMed](#)]
60. Bruno, L.; Talarico, E.; Cabeiras-Freijanes, L.; Madeo, M.L.; Muto, A.; Minervino, M.; Araniti, F. Coumarin interferes with polar auxin transport altering microtubule cortical array organization in *Arabidopsis thaliana* (L.) Heynh. root apical meristem. *Int. J. Mol. Sci.* **2021**, *22*, 7305. [[CrossRef](#)]
61. Li, J.; Xu, H.-H.; Liu, W.-C.; Zhang, X.-W.; Lu, Y.-T. Ethylene inhibits root elongation during alkaline stress through AUXIN1 and associated changes in auxin accumulation. *Plant Physiol.* **2015**, *168*, 1777–1791. [[CrossRef](#)]
62. Soltys, D.; Rudzińska-Langwald, A.; Gniazdowska, A.; Wiśniewska, A.; Bogatek, R. Inhibition of tomato (*Solanum lycopersicum* L.) root growth by cyanamide is due to altered cell division, phytohormone balance and expansin gene expression. *Planta* **2012**, *236*, 1629–1638. [[CrossRef](#)]
63. Steenackers, W.; Klíma, P.; Quareshy, M.; Cesarino, I.; Kumpf, R.P.; Corneillie, S.; Araújo, P.; Viaene, T.; Goeminne, G.; Nowack, M.K. cis-Cinnamic acid is a novel, natural auxin efflux inhibitor that promotes lateral root formation. *Plant Physiol.* **2017**, *173*, 552–565. [[CrossRef](#)]
64. Oono, Y.; Ooura, C.; Rahman, A.; Aspúria, E.T.; Hayashi, K.-i.; Tanaka, A.; Uchimiya, H. p-Chlorophenoxyisobutyric acid impairs auxin response in *Arabidopsis* root. *Plant Physiol.* **2003**, *133*, 1135–1147. [[CrossRef](#)] [[PubMed](#)]
65. De Rybel, B.; Audenaert, D.; Xuan, W.; Overvoorde, P.; Strader, L.C.; Kepinski, S.; Hoye, R.; Brisbois, R.; Parizot, B.; Vanneste, S. A role for the root cap in root branching revealed by the non-auxin probe naxillin. *Nat. Chem. Biol.* **2012**, *8*, 798–805. [[CrossRef](#)] [[PubMed](#)]
66. Blilou, I.; Xu, J.; Wildwater, M.; Willemsen, V.; Paponov, I.; Friml, J.; Heidstra, R.; Aida, M.; Palme, K.; Scheres, B. The PIN auxin efflux facilitator network controls growth and patterning in *Arabidopsis* roots. *Nature* **2005**, *433*, 39–44. [[CrossRef](#)]
67. Swarup, R.; Kramer, E.M.; Perry, P.; Knox, K.; Leyser, H.O.; Haseloff, J.; Beemster, G.T.; Bhalerao, R.; Bennett, M.J. Root gravitropism requires lateral root cap and epidermal cells for transport and response to a mobile auxin signal. *Nat. Cell Biol.* **2005**, *7*, 1057–1065. [[CrossRef](#)]
68. Křeček, P.; Skúpa, P.; Libus, J.; Naramoto, S.; Tejos, R.; Friml, J.; Zažímalová, E. The PIN-FORMED (PIN) protein family of auxin transporters. *Genome Biol.* **2009**, *10*, 249. [[CrossRef](#)] [[PubMed](#)]
69. Muday, G.K.; Murphy, A.S. An emerging model of auxin transport regulation. *Plant Cell* **2002**, *14*, 293–299. [[CrossRef](#)] [[PubMed](#)]
70. Araniti, F.; Bruno, L.; Sunseri, F.; Pacenza, M.; Forgione, I.; Bitonti, M.B.; Abenavoli, M.R. The allelochemical farnesene affects *Arabidopsis thaliana* root meristem altering auxin distribution. *Plant Physiol. Biochem.* **2017**, *121*, 14–20. [[CrossRef](#)]
71. Sun, P.; Tian, Q.-Y.; Chen, J.; Zhang, W.-H. Aluminium-induced inhibition of root elongation in *Arabidopsis* is mediated by ethylene and auxin. *J. Exp. Bot.* **2010**, *61*, 347–356. [[CrossRef](#)]
72. Michniewicz, M.; Zago, M.K.; Abas, L.; Weijers, D.; Schweighofer, A.; Meskiene, I.; Heisler, M.G.; Ohno, C.; Zhang, J.; Huang, F. Antagonistic regulation of PIN phosphorylation by PP2A and PINOID directs auxin flux. *Cell* **2007**, *130*, 1044–1056. [[CrossRef](#)]
73. Dubrovsky, J.G.; Sauer, M.; Napsucialy-Mendivil, S.; Ivanchenko, M.G.; Friml, J.; Shishkova, S.; Celenza, J.; Benková, E. Auxin acts as a local morphogenetic trigger to specify lateral root founder cells. *Proc. Natl. Acad. Sci. USA* **2008**, *105*, 8790–8794. [[CrossRef](#)]
74. Alarcón, M.; Salguero, J.; Lloret, P.G. Auxin modulated initiation of lateral roots is linked to pericycle cell length in maize. *Front. Plant Sci.* **2019**, *10*, 11. [[CrossRef](#)]
75. Casimiro, I.; Beeckman, T.; Graham, N.; Bhalerao, R.; Zhang, H.; Casero, P.; Sandberg, G.; Bennett, M.J. Dissecting *Arabidopsis* lateral root development. *Trends Plant Sci.* **2003**, *8*, 165–171. [[CrossRef](#)]
76. Laskowski, M.J.; Williams, M.E.; Nusbaum, H.C.; Sussex, I.M. Formation of lateral root meristems is a two-stage process. *Development* **1995**, *121*, 3303–3310. [[CrossRef](#)] [[PubMed](#)]
77. Potters, G.; Pasternak, T.P.; Guisez, Y.; Jansen, M.A. Different stresses, similar morphogenic responses: Integrating a plethora of pathways. *Plant Cell Environ.* **2009**, *32*, 158–169. [[CrossRef](#)] [[PubMed](#)]
78. Gniazdowska, A.; Krasuska, U.; Andrzejczak, O.; Soltys, D. Allelopathic compounds as oxidative stress agents: YES or NO. In *Reactive Oxygen and Nitrogen Species Signaling and Communication in Plants*; Springer: Berlin/Heidelberg, Germany, 2015; pp. 155–176.
79. Rudrappa, T.; Bonsall, J.; Gallagher, J.L.; Seliskar, D.M.; Bais, H.P. Root-secreted allelochemical in the noxious weed *Phragmites australis* deploys a reactive oxygen species response and microtubule assembly disruption to execute rhizotoxicity. *J. Chem. Ecol.* **2007**, *33*, 1898–1918. [[CrossRef](#)] [[PubMed](#)]
80. Bais, H.P.; Vepachedu, R.; Gilroy, S.; Callaway, R.M.; Vivanco, J.M. Allelopathy and exotic plant invasion: From molecules and genes to species interactions. *Science* **2003**, *301*, 1377–1380. [[CrossRef](#)] [[PubMed](#)]
81. Rawlinson, C.; Kamphuis, L.G.; Gummer, J.P.; Singh, K.B.; Trengove, R.D. A rapid method for profiling of volatile and semi-volatile phytohormones using methyl chloroformate derivatisation and GC-MS. *Metabolomics* **2015**, *11*, 1922–1933. [[CrossRef](#)] [[PubMed](#)]